第 48 卷 第 9 期
2021 年 9 月

湖南大学学报（自然科学版）
Journal of Hunan University (Natural Sciences)

Vol. 48. No. 9.
September 2021

Open Access Article

Tuberculosis X-Ray Images Classification based Dynamic Update Particle Swarm Optimization with CNN

Marina Yusoff[1,2], Mohamad Syafiq Irfan Saaidi[2], Amirul Sadikin Md Afendi[1], Azrin Mohd Hassan[3]

[1] Institute for Big Data Analytics and Artificial Intelligence, Universiti Teknologi MARA, Selangor, Malaysia

[2] Faculty of Computer and Mathematical Sciences, Universiti Teknologi MARA, Selangor, Malaysia

[3] FOMEMA Sdn Bhd., Jalan Kampung Pandan 55100 Kuala Lumpur, Malaysia

Abstract: The classification of tuberculosis (TB) based on chest X-Ray (CXR) remains a time-consuming activity that requires an expert's interpretation. An automated TB classification on the CXR can be a significant clinical utility to overcome this issue as the disruptive technology is concerned. Most recent research focused on deep learning solutions but identifying the suitable network architecture remains a challenge as it depends on the image features. One of the network architectures is at the classification layer. This paper highlighted a proposed hybrid CNN and enhanced Particle Swarm Optimization (CNN-ePSO) to find an optimal architecture of a connected layer at the classification network layer. We proposed a discrete and real value representation of the particle and a dynamic update strategy of the particle. A series of experiments are performed using Montgomery and Shenzhen CXR for the image classification performance. Formulation of a suitable particle representation has shown a workable particle representation and successfully achieved its aim. The outcome assesses that the hybrid CNN-ePSO with image enhancement is superior to the CNN-PSO without image enhancement and other single CNN models with a remarkable improvement. Thus, a novel ePSO algorithm embedded with CNN captures significant attention on the classification result, mainly for CXR images. In the future, additional work on deep feature layer optimization would be possible for a better result and application of the most recent algorithm like cuckoo search and firefly algorithm.

Keywords: image classification, convolution neural network, deep learning, X-ray Images, particle swarm optimization.

基于结核病 X 射线图像分类的动态更新粒子群优化与美国有线电视新闻网

摘要：基于胸部 X 射线 (CXR) 的结核病分类仍然是一项耗时的活动，需要专家的解释。就破坏性技术而言，CXR 上的自动结核病分类可能是克服这一问题的重要临床效用。大多数最近的研究都集中在深度学习解决方案上，但确定合适的网络架构仍然是一个挑战，因为它取决于图像特征。网络架构之一位于分类层。本文重点介绍了提出的混合美国有线电视新闻网和增强粒子群优化 (美国有线电视新闻网-ePSO)，以在分类网络层找到连接层的最佳架构。我们提出了粒子的离散实值表示和粒子的动态更新策略。使用蒙哥马利和深圳 CXR 对图像分类性能进行了一系列实验。合适的粒子表示的制定已显示出可行的粒子表示并成功实现其目标。结果评估具有图像增强的混合美国有线电视新闻网-ePSO 优于没有图像增强的美国有线电视新闻网-粒子群算法和其他具有显着改进的单个美国有线电视新闻网模型。因此，嵌入美国有线电视新闻网的新型

Received: June 1, 2021 / Revised: June 6, 2021 / Accepted: July 27, 2021 / Published: September 30, 2021

About the authors: Marina Yusoff, Institute for Big Data Analytics and Artificial Intelligence, Universiti Teknologi MARA, Selangor, Malaysia; Faculty of Computer and Mathematical Sciences, Universiti Teknologi MARA, Selangor, Malaysia; Mohamad Syafiq Irfan Saaidi, Faculty of Computer and Mathematical Sciences, Universiti Teknologi MARA, Selangor, Malaysia; Amirul Sadikin Md Afendi, Institute for Big Data Analytics and Artificial Intelligence, Universiti Teknologi MARA, Selangor, Malaysia; Azrin Mohd Hassan, FOMEMA Sdn Bhd., Kuala Lumpur, Malaysia

ePSO 算法在分类结果上引起了极大的关注，主要针对 CXR 图像。未来，在深度特征层优化方面的额外工作将有可能获得更好的结果和应用最新的算法，如布谷鸟搜索和萤火虫算法。

关键词：图像分类、卷积神经网络、深度学习、X 射线图像、粒子群优化。

1. Introduction

Tuberculosis (TB) is an acute infectious disease in the world. Quick and precise TB classification is necessary for ensuring disease prevention. Nonetheless, TB diagnosis disparities continue to exist in many high-burden countries [1]. TB ranks among the top in worldwide fatality causes [2]. Every year millions of people tend to fall ill with TB. In 2018, ten million individuals were approximately infected with TB, and a million and a half have reported the death. The disease implication ranges greatly from fewer than 5 to over 500 new patients per 100 000 citizens every year [3]. The fundamental cause of this high death rate is the gap in TB detection: over one portion of approximately ten million TB incidents is not registered and detected [4]. Many solutions were established. One of them is Chest X-Ray (CXR).

CXR is restricted through its moderate accuracy, overprice equipment, and low reliability. Moreover, some countries with the largest burden share suffer from skilled radiologists' shortage in analyzing the CXR images [1]. An automated CXR TB screening system should be viable for low-income countries with low accessibility to healthcare providers [5]. Deep learning techniques are currently considered because of their excellent rapport in image classification capability. It seems the technique is well suited for image analysis. The research on deep learning capabilities is still ongoing, especially in medical and healthcare. Deep learning work in the classification of medical images has produced results that match medical experts. In a data collection of over 100,000 CXR, CheXNet has shown an improved solution to radiologists offering assistance [6]. The diagnosis of pulmonary TB on CXR declared impressive introductory output analyses of five hundred people infected with TB and about five hundred ordinary people in four data collection by utilizing convolution neural network (CNN) methods. Even so, their work was centralized on identifying TB with limited data collection [7]. More work was done on a specific CXR image and demonstrated different results with many deep learning models and multiple types of CXR images, including COVID-19 CXR images [8-9]. However, it is a problem [8] and architecture [9-10] and parameters dependence [7], [12]. Also, the quality of the X-Ray images requires a specific task like augmentation [6], [9] to deal with a small number of images and images enhancement [13] and to remove noise or related occlusion [12].

Another important aspect is the applied classification method that determines the accurateness of the solution. Different architectures of CNNs can influence the CNN model performances. Identifying suitable architecture remains a challenge as it is the dependent type and features of the images. Recent research produced and tested on deep learning solutions improved the solutions with several strategies such as transfer learning and embedded nature-inspired algorithms [12], [15]. Several aspects were considered when employed nature-inspired algorithms, such as one of the popular [16-17], easy implementation [18-20], and fast convergence [19] is Particle Swarm Optimization (PSO). PSO has successfully searched for optimal network architectures [10-11], [21-22]. For instance, PSO can work as an autoencoder for CNN architectures-based image classification architectures [10-11], [21]. However, their algorithm deals with searching an optimal convolution architecture in CNN using Shenzen (SZ) and Montgomery County (MC) benchmark CXR datasets. The accuracy was reported to improve with the employment of PSO. In this paper, we concentrate on the steps for finding a suitable classification layer. In this respect, a nature-inspired computational optimization is improved to accommodate mainly adaptive changes of several layers.

Hence, we proposed an enhanced PSO (ePSO) that is hybrid with CNN. The CNN-ePSO is expected to find an optimal architecture of a connected layer at the classification layer. The comparison with the recent CNN model and the previous models using benchmark TB CXR images is elaborated. We aim to use PSO to select the network layer architectures with a good balance between searching, loss, and classification accuracy. Thus, our main contribution is a novel PSO algorithm is proposed for an optimal architecture in classifier layers selection using dynamic particles update with certain ranges. Particles are allowed to grow and reduce in size with an upper bound and lower bound, respectively.

This article is arranged to start with Section 2 explains the related work on CNN and PSO. Material and methods are presented in Section 3. Section 4 discusses the computational results and a comparison with the chosen algorithm and discussion. Finally, Section 5 presents a conclusion and proposes a research direction for future works.

2. Research Background

A few approaches to computational studies have been earlier stated to classify lung diseases. For instance, a computational system utilizes Support Vector Machine (SVM), classifying Computer Tomography (CT) lung images into malignancy [23], and deep CNN methods [24]. CNN is becoming the most common algorithm for X-Ray image classification in many domains [24-26].

The CNN method also was introduced by Hattikatti to identify interstitial lung disease of the 2D CT image of the lung by utilizing Local Binary Pattern (LBP) characteristics [27]. The patch CNN method was used in [28]to classify the normal and other lung tissue classes. Different performances were reported in the use of CNN using various types of X-Ray images. Thus, 87% accuracy was obtained in [29], while 85.29% accuracy was obtained in [15] considering differences in the CNN architectures and datasets. Three separate optimization models were tested in [30] and it was discovered that the Adam optimization model overpowers the others by accomplishing 94.73% accuracy in training and 82.09% accuracy in testing. They used a simple multi-layered architecture, LeNet, and Alexnet architectures and tested the CXR of MC and SZ datasets. Few architectures were tested; however, it can be seen that VGG19 was better than the other methods with optimized functions [31]. Image pre-processing, image augmentation, genetic algorithm-dependent hyperparameter tuning, and model assembling were utilized for segmenting and classifying lungs CXR [5]. The outcomes have shown a significant improvement. Another possible aspect is the use of the Bayesian convolutional neural network (B-CNN). The findings show that B-CNN outperforms CNN [32].

In obtaining better results, one aspect is transfer learning. Past research shows that utilizing the ImageNet dataset pre-trained network, then fine-tune it to a more particular dataset, produces excellent results in the classification and detection process [33-35]. This training protocol is booming because CNN receives the overall ability for description from natural image pretraining. Model adjusted the parameter after fine-tuning to represent specific characteristics of particular images and maintain the ability to display images. Many efforts in analyzing different CNN techniques, learning variables, and transfer learning for the TB CXR dataset were made in [36]. TB CXR images were detected by fine-tuning the pre-trained CNN system using the clinical natural image data collection CXR image on architectures from AlexNet and GoogLeNet. The model was trained using imbalanced data collection. Shuffle sampling utilizes the augmentation of data collection, increasing the precision of AlexNet by 53.02 % to 85.68 % and the accuracy of GoogleNet from 56.11 % to 91.72 %. ImageNet weight-train InceptionV3 and transfer learning from OCT images of 108,312 datasets were utilized in [37], resulting in an average of 96.6 % accuracy, 97.8 % sensitivity, and 97.4 % specificity. They evaluated the findings with several experts. The findings have high sensitivity but low specificity, while increased sensitivity and high specificity values were found in the deep learning model.

Fine-tuning the model with multiple data augmentation techniques has shown good potential. In dealing with augmentation, pre-processing, data enhancement, image segmentation is used to classify CXR images, and segmented images of the lung obtained good results with CNN models [38]. It is interesting to note that augmentation processes can be established to add more datasets considering a few angles of images and have a high chance of getting better performances when we lack images.

The hybrid CNN and PSO were used in improving images classification performances [21], [39]. PSO mostly worked best for hyperparameter selection [40-42] and selection of convolution in deep neural networks [21], [39]. There are cases, for instance, where PSO is embedded with CNN and XGBoost to find the best parameter for COVID-19 diagnosis classification [39]. The work has resulted in a better performance compared to CNN and XGboost. Most of them use PSO for hyperparameter tuning selection and finding an optimal convolution network architecture compared to the selection of neural network architecture in a classifier stage. The use of PSO has demonstrated a better performance in the classification of CXR images. Thus, we can conclude that PSO can be designed to suit the requirement of improvement for the CNN, especially in TB CXR images

3. Material and Method

The structure of the proposed TB CXR images classification approach is illustrated in Fig.1, and the following steps summarize this structure. The first stage is data preparation and augmentation using a set of methods elaborated in Section 3.1.

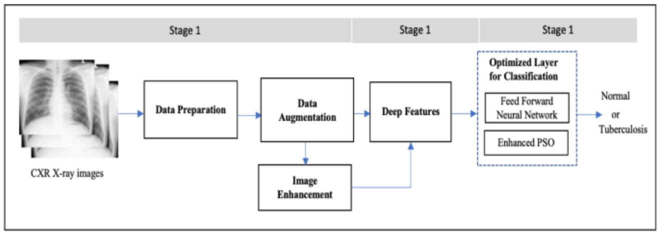

Fig. 1 The structure of CNN-PSO TB. CXR classification approach

As shown in Fig. 1, the image enhancement task is added to see the performance comparison between original and enhanced images. The second stage is to extract features using a set of CNN models. The third stage is to classify the relevant features extracted by the CNN models.

3.1. Data Preparation

Since TB data is very confidential, and the diagnosis of TB with a gold standard is complex, the openly accessible TB datasets are restricted and limited. We use two CXR datasets on TB CXR, MC, and SZ datasets [21]. MC CXR is made up of 138 CXR images, in which there are 80 positive cases, while 58 are cases with TB. Meanwhile, SZ CXR datasets comprise 326 positive and 336 TB manifestations, resulting in 662 CXR images. The image is labeled as vectors containing the value “1” in the positive TB category and the value “0” in the other category. For the evaluation, a total of 800 CXR images were used to classify the TB model to classify whether the CXR is normal or TB. The dataset was separated into 85:15 ratio. Hence, 680 was used for training and 120 for validation and testing purposes.

3.2. Data Augmentation

The augmentation method aims to increase the training dataset size to help identify hidden patterns in the original CXR image. It is expected to decrease the probabilities of overfitting the model. Augmentation is done using the TFLearn Data Augmentation available in TensorFlow [43]. Due to size and graphic processing power shortcomings, an augmentation in the random size of batch 50 from the training dataset was applied. The rescaling process is done to get the input images in the range of zero to one. A pixel between 0 and 255 creates each digital image, 0 in black and 255 in white. So, rescale the scale array of the original image pixel values between 0 and 1, making the images contribute more evenly to the overall loss. Otherwise, a higher pixel range image results in higher losses, and a lower learning rate should be used, and a lower pixel range image will need a higher learning rate. Fig. 2 shows the augmented CXR images after the augmentation process and will be used for training purposes. We use augmentation image generation based on width shift, height shift, the zoom range of 0.05, and rotation range equal to 5.0.

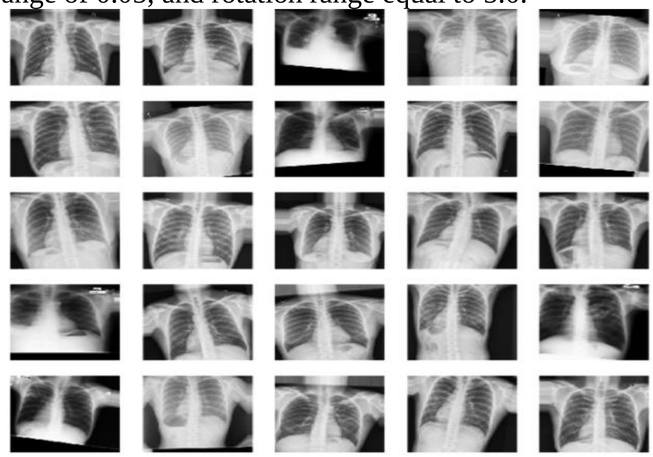

Fig. 2 Example of augmented CXR used for training

3.3. Image Enhancement

Contrast Limited Adaptive Histogram Equalization (CLAHE) as an image enhancement method employed as it was reported good performance for X-Ray images [44]. It offers a better prominent structure of the images. Fig. 3 demonstrates a sample of enhanced TB CXR images.

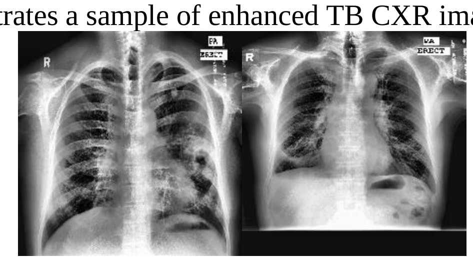

Fig. 3 Example of enhanced TB CXR image with CLAHE

3.4. Deep Features Extraction with CNN

CNN is influenced by animal and human cortex visual identification used for applications, including recommendation systems and image and video recognition. CNN architectures openly assume that the inputs involve images, allowing the architecture to encode specific properties. In this section, we explain one of the recent models, VGG19 [45]. The VGG19 is a part of the VGG model that consists of 19 layers-based CNN models. The input layer contains the width, height, and dimension of the input image. CNN’s neuron is a 3D filter that activates following the inputs. They are only linked with a small region of a previous neuron activation, known as the receptive field. The convolution process is computed between inputs and parameters and gets activated based on the output and non-linearity function. The CNN layers are classified into three types: convolutional, pooling, and fully connected layers. The convolutional layer is the CNN's building block. It is essential to consider that the parameters of the layers consist of trainable neurons or filters. The network learns to produce filters when it senses a specific feature type at a location within the input features map, creating a weighted sum features map [46].

Pooling layers control width by measuring height by lowering spatial dimension of the input volume for the next convolutional layer without changing the dimensional depth. The fully connected layer is then converted into a 1D feature vector. Furthermore, the vector generated in this phase is classified for classification class or further processing of the feature vector. The VGG19 architecture starts with five blocks of a convolutional layer in which consists of connected layers. Convolutional layers utilized 3 × 3 kernels.

Flatten are used between the fully connected layer by modifying a two-dimensional matrix to a one-dimensional matrix as it can be used in the fully connected layer. SoftMax activation function with the cross-entropy loss is used to convert output neurons to a probability between 0 and 1 based on which class the images belong to. Binary cross-entropy loss is utilized because the TB CXR dataset only contains 0 for normal and 1 for TB cases. The Adam optimizer is chosen because its performance outperforms the other optimizer in research [30].

3.5. Enhanced Particle Swarm Optimization

Particle Swarm Optimization (PSO) is the popular metaheuristic and stochastic algorithm. It was introduced in mid-1995, originally solving the binary problem [47]. The original PSO steps can be found in various publications [48-49]. Many variants were enhanced and established, including its representation of particle and hybridization complementing other methods [21], [39]. The PSO helps improve the solution towards an optimal solution for an optimization problem. One of its capabilities is in parameter tuning and control but requires a suitable representation of particles as it is important to run the PSO [21], [49-50]. In the aspect of the CNN solution, this paper addresses the use of PSO in finding the most suitable layers of the neural network of the classifier.

TB CXR images classification addresses the objective function of finding the minimum loss and high accuracy concerning deep method employment. To obtain a better solution, selecting a suitable layer is necessary. We used a discrete PSO implementation and followed the initial steps of PSO [47]. Fig. 4 is the representation of the particle, L = {L1, L2, L3, …Ln} and Dropout, DP={0.1, 0.2, 0.3, 0.4, 0.5.

L_1	L_2	…	L_n	DP

Fig. 4 Particle representation for neural network architecture and dropout

Each component in the particles consists of layers that are randomly initiated in a population. Discrete value for all layers is initiated as stated in Equation 1.

$$d = rand(x,y)*z \quad (1)$$

where x,y, and z = index of layer calculation, x ={1, 2, 3…m}.

Equation 2 and Equation 3 present the velocity and position formulas for the discrete PSO, respectively.

$$V_{id(new)}=W * V_{id} + C_1 r_1 * (Pbest_{(id)} - X_{id} + C_2 * r_2 * (Gbest_{(id)}-X_{id}) \quad (2)$$

$$X_{id(new)}=X_{id} + V_{id(new)} \quad (3)$$

where:
$V_{id(new)}$ = new velocity
V_{id} = current velocity
X_{id} = curren position
$X_{id(new)}$ = new position
W = inertia weight
C_1 and C_2 = acceleration coefficient
r_1 *and* r_2 = random function
$Pbest_{(id)}$ = position of the personal best
$Gbest_{(id)}$ = position of the global best

We introduced a particle update based on this procedure. Particle update is adjusted during iterations to find the best fit model of the network. The dynamic range update is based within +8 or -8 for all L values, and DP is an increased value of 0.1. The PSO algorithms are as illustrated in Algorithm 1: Enhanced PSO. A canonical PSO is modified to suit the solution representation to obtain the most suitable layers of feed-forward neural network. The modification covers the initialization of discrete particle position, considering the expected number of discrete particle values at each layer.

Algorithm 1: ePSO

Begin
Set the population size P, the maximum number of iterations I.
Initialize random populations for each particle
Declare W, C_1, and C_2
Initialize $V_{id(min)}$ and $V_{id(max)}$
Initialize $Xi_{d(min)}$ and $Xid_{(max)}$
Calculate Pbest and Gbest value for each particle
Do
  For each particle
    Calculate new velocity value, $V_{(new)}$
    Calculate new position, $D_{(new)}$
    Calculate Pbest $_{(new)}$
    Calculate Gbest $_{(new)}$
    For each particle dimension
      If current Pbest ≥ current Gbest

New particle dimension = current particle dimension – particle change value
If current Pbest < current Gbest
New particle dimension = current particle dimension + particle change value
While (stopping condition is reached)
End

3.6. Evaluation Metrics

Evaluation of the method was referred to as the confusion matrix score, which is popular in model validation, especially in medical images [51]. The accuracy, precision, recall, and F1-Score were used to evaluate all models. Accuracy is calculated based on the predictions made by the model. It is divided by the total number of predictions.

Besides, a loss is an additional evaluation when evaluating the CNN-PSO. Loss is a distance between the actual and predicted value produced by the model. The greater the loss value is evident more errors. The function used to calculate the loss value is a sparse categorical cross-entropy function [52].

4. Results for Computational Experiment and Discussion

This section highlights the comparisons of the CNN models and a proposed CNN-PSO model.

4.1. Comparison Results of the CNN Models

This section evaluates five CNN models: Mobile Net, Xception, ResNet50, InceptionV3, and VGG19. The models are the most commonly used in imaging classification with deep learning. When comparing model performance, the evaluation metrics such as accuracy, F1 score, precision, and recall were used to evaluate the model. The comparisons of the accuracy among five pre-trained models are shown in Figure 5 (a), (b), (c), (d), (e), respectively.

In the evaluation, trial-and-error method of the hyperparameters settings of the five different pre-trained CNN models using the validation dataset. The learning rate of all the five different pre-trained CNN models is reduced until the minimum of 0.00001. For the VGG19 model, the training dataset is split into ten batches. The model used 100 epochs. The initialized weights of ImageNet are used for each layer. The weight value was updated using Adam Optimizer for each epoch. The learning rate is reduced to a minimum of 0.00001. VGG19 obtained the maximum probabilities of validation accuracy of 0.91 from 0 to 1 on the test dataset. VGG19 model used 6,423,298 trainable layers parameter and 20,024,384 non-trainable parameters of VGG19 layers. Regarding the MobileNet model, the training dataset is split into ten batches. The initialized weights of ImageNet are used for each layer. The learning rate is reduced to a minimum of 0.00001. MobileNet obtained the second-highest validation accuracy probability of 0.88 from 0 to 1 on the test dataset. MobileNet model used 12,845,846 trainable layers parameter and 3,228,864 non-trainable parameters of MobileNet layers.

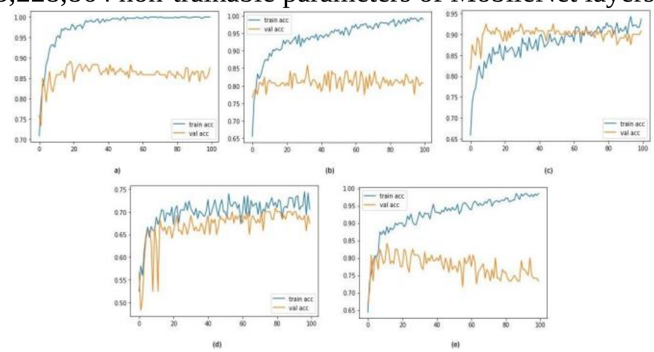

Fig. 5 Accuracy comparison of five pre-trained CNN models with (a) MobileNet, (b) Xception, (c) VGG19, (d) ResNet50, (e) InceptionV

The Xception model has the same datasets and parameters as the VGG19 and MobileNet parameters. The weights of ImageNet were also used for each layer. Xception comes in third place behind VGG19 and MobileNet, with a validation accuracy of 0.81 from 0 to 1 probability on the test dataset. The Xception model utilized 25,690,882 trainable layers parameter and 20,861,480 non-trainable parameters of Xception layers. For the InceptionV3 model, the training data set parameters are also the same as the other model parameters. The weights of ImageNet were also used for each layer. InceptionV3 ranks fourth among all five pre-trained CNN models, achieving a test dataset probability validation accuracy of 0.73 from 0 to 1. InceptionV3 model operates with 13,107,970 trainable layers parameter and 21,802,784 non-trainable parameters of InceptionV3 layers. In the ResNet50 model, the parameters used for the training dataset are also the same as the other model parameters. The weights of ImageNet were also used for each layer. ResNet50 ranks fifth behind all four pre-trained CNN models, achieving a probability validation accuracy of 0.68 from 0 to 1 on the test dataset. ResNet50 model used 25,690,882 trainable layers parameter and 23,587,712 non-trainable parameters of ResNet50 layers.

ImageNet supplies the weight knowledge to the CNNs. The summary of all evaluation metrics measurements is in Table 1, including the accuracy, F1 score, precision, and recall values. The highest evaluation metrics currently provided by VGG19 are 0.91 on the accuracy, 0.91 on the F1 score, 0.92 on Precision, and 0.91 on Recall. It can be concluded from the classification results that the VGG19 model showed better performance than all the other pre-trained CNN models, including MobileNet, ResNet50, InceptionV3, and Xception. The accuracy of the VGG19 model is the highest at 0.91 and the lowest in the ResNet50 model with 0.68. Although the other pre-trained CNN model did not achieve better accuracy than the VGG19 model, the network complexity differs between the VGG19 model and other pre-trained CNN models.

Table 1 Performance measure of all CNN models

Particle	L_1	L_2	L_3	L_4	DP	Loss	Accuracy
A_1	232	152	64	168	0.3	0.26	0.92
A_2	48	96	64	144	0.3	0.26	0.94
A_3	152	72	64	184	0.3	0.26	0.94
A_4	144	80	176	216	0.4	0.27	0.94
A_5	208	120	200	232	0.3	0.36	0.92
A_6	208	232	144	152	0.4	0.23	0.92
A_7	40	96	216	144	0.3	0.27	0.92
A_8	208	160	144	216	0.3	0.31	0.92
A9	48	136	168	88	0.3	0.37	0.94
A10	40	72	168	40	0.3	0.37	0.92

This research presented a CNN model that uses VGG19 to classify the CXR images to identify patients with TB. Previous CXR classification research applied complex lung segmentation models before training the model using support vector machines. This research shows that the VGG19 model can use raw data to identify the results with comparable accuracy without any lung segmentations performed in the previous research. To further improve the accuracy, the VGG19 model was applied on a sequential model. A flatten and dropout layer was also added to the fully connected layer to see whether the model achieved 91% accuracy. It is demonstrated that VGG19 achieved a better accuracy of about 10% higher compared to the other four models. In the next section, we explain the computational results of the proposed solution.

4.2. Performance of CNN-ePSO Using Original Images

In this experimental evaluation, we use the same set of the parameter of VGG19. The modification part of the CNN is the classification layer. The minimum layer of L = 6 and the maximum of L =256 were considered. Here, a dynamic update particle of -8 or +8 is established based on the fitness of the solution. We run CNN-PSO with ten population sizes for five iterations. We follow the classical choice of population size that requires only a low number of sizes [52]. The weight is 0.9, as suggested in [47], [49]. The velocity and position value range are between 0 and 1. The dropout value is randomly initialized and update dynamically within the range of 0.1 and 0.5. The dropout dynamic update value is either -0.1 or +0.1. In this case, we use four layers of networks. Table 2 shows the result of CNN-ePSO at the 1st iteration with ten particles that generated ten classification layers. The results were based on the use of original images.

Interestingly, particle A_1 outperforms other particles, and most of the accuracy is better than CNN-VGG19, as demonstrated in Table 1. There are four particles reported at the highest accuracy of 94%. The highest loss value is obtained by particle A_4, but the accuracy s only 92%. The results suggest that the embedded PSO in the fully connected layer gives an added value mainly in the model accuracy. Particles A_2 and A_3 achieved the highest accuracy of 94% and a lower value than A_1, as indicated in Table 2. At the 5th iteration, as demonstrated in Table 3, all particles obtained more than 92% accuracy.

Table 2 Results of CNN-PSO with original images at the 1st iterations

Particle	L_1	L_2	L_3	L_4	DP	Loss	Accuracy
A_1	256	160	48	160	0.3	0.30	0.94
A_2	32	96	48	128	0.2	0.36	0.94
A_3	160	48	48	176	0.3	0.25	0.92
A_4	144	64	192	224	0.2	0.23	0.92
A_5	224	128	224	256	0.2	0.38	0.94
A_6	224	256	144	144	0.2	0.25	0.92
A_7	16	96	240	128	0.2	0.25	0.91
A_8	224	176	144	224	0.2	0.40	0.95
A9	32	144	176	64	0.2	0.33	0.92
A10	16	48	176	16	0.2	0.36	0.94

Table 3 Results of CNN-PSO with original images at the 5th iterations

Measure	Mobile Net	Xception	Res Net 50	Inception V3	VGG 19
Accuracy	0.88	0.81	0.68	0.73	0.91
F1 Score	0.88	0.81	0.68	0.73	0.91
Precision	0.88	0.81	0.68	0.74	0.92
Recall	0.87	0.81	0.67	0.73	0.91

4.3. Performance of CNN-ePSO Using Enhancement Images

In this section, we explain the performance of CNN-PSO using enhanced images. The same setting is employed, as mentioned earlier. Results of CNN-PSO with image enhancement at the 1st iteration are illustrated in Table 4. The utilization of an enhancement image has resulted in a significant improvement in its performance. All particles have demonstrated a significant improvement in accuracy from 94% to 97%. In terms of loss value, all particles obtained less value than the performance in Section 4.2. The highest loss value was reduced to a minimum of 0.09, as indicated by the A10 particle. At the 5th iteration, particle A_7 finally achieved the highest accuracy, 98%, at the same loss value of 0.09 as demonstrated in Table 5.

Table 4 Results of CNN-PSO with image enhancement at the 1st iterations

Particle	L_1	L_2	L_3	L_4	DP	Loss	Accuracy
A_1	16	16	112	96	0.3	0.19	0.97
A_2	72	168	56	96	0.2	0.2	0.97
A_3	40	232	104	232	0.2	0.13	0.95
A_4	200	24	152	136	0.2	0.14	0.97
A_5	72	184	136	232	0.3	0.14	0.97
A_6	16	136	88	168	0.2	0.15	0.95
A_7	56	136	216	24	0.2	0.13	0.97
A_8	40	56	200	56	0.2	0.12	0.97
A_9	16	232	216	88	0.2	0.11	0.97
A_{10}	248	72	168	56	0.3	0.09	0.97

Table 5 Results for CNN-PSO with image enhancement at the 5th iterations

Particle	L_1	L_2	L_3	L_4	DP	Loss	Accuracy
A_1	16	16	112	96	0.06	0.21	0.97
A_2	56	152	72	96	0.10	0.24	0.97
A_3	24	216	112	216	0.13	0.12	0.97
A_4	184	16	136	120	0.35	0.14	0.97
A_5	56	168	120	216	0.56	0.11	0.97
A_6	16	120	104	152	0.5	0.16	0.97
A_7	40	120	200	40	0.85	0.09	0.98
A_8	24	40	184	72	0.12	0.14	0.97
A9	16	216	200	96	0.00	0.14	0.97
A10	232	56	152	72	0.46	0.16	0.97

4.4. Comparison Performance of CNN-PSO, CNN Models and a Recent Solution

This section gives some important points obtained from the results of the experiments. It was based on the capability of both CNN and PSO. CNNs play an essential role in many imaging domains, especially in healthcare solutions. Thus, to validate our proposed CNN-PSO, we compare it against CNN models. The result is shown in Table 6. Overall, the stochastic flavor of PSO led to a better classification performance with a 3% improvement in accuracy, F1 Score, Precision, and Recall as compared to VGG19 of the CNN model when using original images. However, a significant result is achieved using enhanced images with 98% accuracy, F1 Score, Precision, and Recall. The dynamic particle update of the layer and dropout give an effect on the accuracy and loss.

Table 6 Comparison performance of CNN-PSO and CNN models

Measurement	CNN-VGG19	CNN-ePSO (Original images)	CNN-ePSO (Enhanced images)
Accuracy	0.91	0.94	0.98
F1 Score	0.91	0.94	0.98
Precision	0.92	0.96	0.98
Recall	0.91	0.94	0.98

Compared to VoPreCNNFT developed in [13], the proposed CNN-PSO with CLAHE performed about a similar result which is 98% accuracy. However, their evaluation on the separate datasets of MC and SZ. It is supported that the chosen fully connected layer architecture is one of the criteria for the image classification performance [21]. PSO itself has shown its capability in finding the optimized architecture. The balance of exploitation and exploration searching strategy in PSO has brought a good result even with only five iterations. Even though a small population size is used, the result is at par compared to the recent output from [13]. In addition, evaluation of PSO can be extended by using more numbers of population size as also suggested by [53].

5. Conclusions

This paper presents the proposed CNN-ePSO models to handle automated TB CHR image classification challenges. CNN, to be known, requires many images for its training task. Producing adequate experimental datasets in the real world is challenging. In this work, the augmentation processes for the existing images were performed to improve identifying its features before applying the models. The benchmark TB CXR images were used to perform a binary classification, whether it falls under normal or TB. The VGG19 with appropriate dense layer and dropout parameters are evident for better performance than MobileNet, ResNet50, InceptionV3, and Xception, with the same datasets and augmentation images. A different architecture of CNNs and training parameters influence the CNN model performances. The CNN-ePSO with image enhancement has demonstrated superior performance in accuracy and loss. A novel ePSO as an embedded tool to CNN was reported as a significant commitment to all CNN methods. ePSO has performed well with a small number of population sizes in this context, as proved in many types of problems. Also, PSO works well in balancing the global and local search that aims for an optimal solution. Hence, the proposed CNN-ePSO can be tested on different types of CXR especially using real-life data. It is expected to provide good accuracy.

In addition, some limitations such as the performance on computational times and lack of concentration in deep feature behavior could be improved using several strategies. Future work can improve efficiency by adding embedded optimization algorithms such as the most recent Cuckoo Search and firefly algorithm. Another part of improvement is enhancing the feature extraction at the convolution layer, such as ensemble methods. For instance, this research can be made more effective by implementing a hybrid method. The pre-processed CXR image can be used and further processed where the region of interest can be extracted from these CXR images.

Acknowledgment

The authors would like to thank FOMEMA Sdn. Bhd. for the funding the research on Development of Artificial Intelligence (AI) Teleradiology Software Solutions for Digital X-Ray Reading and the Institute for Big Data Analytics and Artificial Intelligence (IBDAAI) and Faculty of Computer and Mathematical Sciences, Universiti Teknologi MARA, Shah Alam, Malaysia for the tremendous support.

References

[1] NASH M., KADAVIGERE R., ANDRADE J, *et al.* Deep learning, computer-aided radiography reading for tuberculosis: a diagnostic accuracy study from a tertiary hospital in India. *Scientific Reports*, 2020, 10(1):1-10.

[2] DUONG L. T., LE N. H., TRAN T. B, et al. Detection of Tuberculosis from Chest X-ray Images: Boosting the Performance with Vision Transformer and Transfer Learning. *Expert Systems with Applications*, 2021:115519.

[3] Global Tuberculosis Report 2019, Retrieved on January 22, 2021, from https://www.who.int/teams/global-tuberculosis-programme/tb-reports/global-report-2019.

[4] QIN Z. Z., SANDER M. S., RAI B, et al. Using artificial intelligence to read chest radiographs for tuberculosis detection: A multi-site evaluation of the diagnostic accuracy of three deep learning systems. *Scientific Reports*, 2019, 9(1):1-10.

[5] DASANAYAKA C., and DISSANAYAKE M. B. Deep Learning Methods for Screening Pulmonary Tuberculosis Using Chest X-rays. *Computer Methods in Biomechanics and Biomedical Engineering: Imaging & Visualization*, 2020:1-11.

[6] YADAV S. S., and JADHAV S. M. Deep convolutional neural network based medical image classification for disease diagnosis. *Journal of Big Data*, 2019, 6(1):1-18.

[7] HWANG E. J., PARK S., JIN K. N, *et al*. Development and validation of a deep learning–based automated detection algorithm for major thoracic diseases on chest radiographs. *JAMA Network Open*, 2019, 2(3): e191095-e191095.

[8] KARNKAWINPONG T., and LIMPIYAKORN Y. Classification of pulmonary tuberculosis lesion with convolutional neural networks. *Journal of Physics: Conference Series*, 2019, 1195: 012007.

[9] SENSUSIATI A. D., PRAMULEN A. S., RUMALA D. J, *et al*. A New Approach to Detect COVID-19 in X-Ray Images of Indonesians. *Journal of Hunan University Natural Sciences*, 2021:48(6).

[10] WANG B., SUN Y., XUE B., A and ZHANG M. Evolving deep convolutional neural networks by variable-length particle swarm optimization for image classification. *Proceedings of the 2018 IEEE Congress on Evolutionary Computation* (CEC), 2018: 1-8.

[11] SUN Y., XUE B., ZHANG M., and YEN G. G. A particle swarm optimization-based flexible convolutional autoencoder for image classification. *IEEE Transactions on Neural Networks and Learning Systems*, 2018, 30(8): 2295-2309.

[12] ALCANTARA M. F., CAO Y., LIU B., *et al.* eRx – A technological advance to speed-up TB diagnostics. *Smart Health*, 2020: 16.

[13] TASCI E., ULUTURK C., and UGUR A. A voting-based ensemble deep learning method focusing on image augmentation and preprocessing variations for tuberculosis detection. *Neural Computing and Applications*, 2021: 1-15.

[14] YADAV O., PASSI K., and JAIN C. K. Using deep learning to classify X-ray images of potential tuberculosis patients. *Proceedings of the 2018 IEEE International Conference on Bioinformatics and Biomedicine* (BIBM), 2018: 2368-2375.

[15] GAO X. W., JAMES-REYNOLDS C., and CURRIE E. Analysis of tuberculosis severity levels from CT pulmonary images based on enhanced residual deep learning architecture. *Neurocomputing*, 2020, 392: 233-244.

[16] YARAT S., SENAN S., and ORMAN Z. A Comparative Study on PSO with Other Metaheuristic Methods. In *Applying Particle Swarm Optimization*, Springer, Cham, 2021: 49-72.

[17] TIWARI H., and MADHUMALA R. B. A Review of Particle Swarm Optimization in Cloud Computing. *Smart IoT for Research and Industry*, 2022: 93-108.

[18] SHIRLY A. D., SUDHILAYA M., and PRIYADHARSHINI Y, *et al*. Improving Efficiency and Power Loss Minimization in Landsman DC-DC Converter using Particle Swarm optimization Technique (PSO). *Proceedings of the 2021 2nd International Conference for Emerging Technology* (INCET), IEEE, 2021: 1-6.

[19] LIU W., WANG Z., ZENG N, *et al*. A PSO-based deep learning approach to classifying patients from emergency departments. *International Journal of Machine Learning and Cybernetics*, 2021, 12(7): 1939-1948.

[20] ESCOBAR H., and CUEVAS E. Implementation of Metaheuristics with Extreme Learning Machines. In *Metaheuristics in Machine Learning: Theory and Applications*, Springer, Cham, 2021: 125-147.

[21] JUNIOR F. E. F., and YEN G. G. Particle swarm optimization of deep neural networks architectures for image classification. *Swarm and Evolutionary Computation*, 2019, 49: 62-74.

[22] LAWRENCE T., ZHANG L., LIM C. P, *et al*. Particle Swarm Optimization for Automatically Evolving Convolutional Neural Networks for Image Classification. *IEEE Access*, 2021, 9: 14369-14386.

[23] MANIKANDAN T., and BHARATHI N. Lung cancer detection using fuzzy auto-seed cluster means morphological segmentation and SVM classifier. *Journal of Medical Systems*, 2016, 40(7): 1-9

[24] KHAN A. I., SHAH J. L., and BHAT M. M. CoroNet: A deep neural network for detection and diagnosis of COVID-19 from chest x-ray images. *Computer Methods and Programs in Biomedicine*, 2020, 196: 105581.

[25] YU D., ZHANG K., HUANG L, *et al*. Detection of peripherally inserted central catheter (PICC) in chest X-ray images: A multi-task deep learning model. *Computer Methods and Programs in Biomedicine*, 2020, 197: 105674.

[26] SU Y., LI D., and CHEN X. Lung Nodule Detection based on Faster R-CNN Framework. *Computer Methods and Programs in Biomedicine*, 2021, 200: 105866.

[27] HATTIKATTI P. Texture based interstitial lung disease detection using convolutional neural network. *Proceedings of the 2017 International Conference on Big Data, IoT and Data Science* (BID), IEEE, 2017: 18-22.

[28] ANTHIMOPOULOS M., CHRISTODOULIDIS S., EBNER L, et al. Lung pattern classification for interstitial lung diseases using a deep convolutional neural network. *IEEE Transactions on Medical Imaging*, 2016, 35(5): 1207-1216.

[29] LIU X., LEI H., and HAN S. Tuberculosis Detection from Computed Tomography with Convolutional Neural Networks. *Advances in Computed Tomography*, 2019, 08(04): 47–56.

[30] HOODA R., SOFAT S., KAUR S, *et al*. Deep-learning: A potential method for tuberculosis detection using chest radiography. *Proceedings of the 2017 IEEE International Conference on Signal and Image Processing Applications* (ICSIPA), IEEE, 2017: 497-502.

[31] RAJARAMAN S., CANDEMIR S., XUE Z, *et al*. A novel stacked generalization of models for improved TB detection in chest radiographs. *Proceedings of the 2018 40th Annual International Conference of the IEEE Engineering in Medicine and Biology Society* (EMBC), IEEE, 2018: 718-721.

[32] ABIDEEN Z. U., GHAFOOR M., MUNIR K, *et al*. Uncertainty assisted robust tuberculosis identification with Bayesian convolutional neural networks. *IEEE Access*, 2020, 8: 22812-22825.

[33] CAO Y., LIU C., LIU B, et al. Improving tuberculosis diagnostics using deep learning and mobile health technologies among resource-poor and marginalized communities. *Proceedings of the 2016 IEEE first international conference on connected health: applications, systems and engineering technologies* (CHASE), IEEE, 2016: 274-281.

[34] SHIN H. C., ROTH H. R., GAO M, *et al*. Deep convolutional neural networks for computer-aided detection: CNN architectures, dataset characteristics and transfer learning. *IEEE Transactions on Medical Imaging*, 2016, 35(5): 1285-1298.

[35] TAJBAKHSH N., SHIN J. Y., GURUDU S. R., *et al*. Convolutional neural networks for medical image analysis: Full training or fine-tuning? *IEEE Transactions on Medical Imaging*, 2016, 5(5): 1299-1312.

[36] LIU C., CAO Y., ALCANTARA M, *et al*. TX-CNN: Detecting tuberculosis in chest X-ray images using convolutional neural network. *Proceedings of the International Conference on Image Processing*, ICIP, 2018: 314–318.

[37] KERMANY D. S., GOLDBAUM M., CAI W., *et al*. Identifying Medical Diagnoses and Treatable Diseases by Image-Based Deep Learning Resource Identifying Medical Diagnoses and Treatable Diseases by Image-Based Deep Learning. *Cell*, 2018, 172(5): 1122-1131.

[38] RAHMAN T., KHANDAKAR A., KADIR M. A. *et al*. Reliable tuberculosis detection using chest X-ray with deep learning, segmentation, and visualization. *IEEE Access*, 2020, 8: 191586-191601.

[39] DIAS JÚNIOR D. A., DA CRUZ L. B., BANDEIRA DINIZ J. O, *et al*. Automatic method for classifying COVID-19 patients based on chest X-ray images, using deep features and PSO-optimized XGBoost. *Expert Systems with Applications*, 2021: 183.

[40] GASPAR A., OLIVA D., CUEVAS E., *et al*. Hyperparameter Optimization in a Convolutional Neural Network Using Metaheuristic Algorithms. In *Metaheuristics in Machine Learning: Theory and Applications*. Springer, Cham. 2021: 37-59.

[41] FOYSAL M. F. A., SULTANA N., RIMI T. A., and RIFAT M. H. Convolutional Neural Network Hyper-Parameter Optimization Using Particle Swarm Optimization. In *Emerging Technologies in Data Mining and Information Security*, Springer, Singapore, 2021: 363-373.

[42] TUBA E., BAČANIN N., STRUMBERGER I., and TUBA M. Convolutional Neural Networks Hyperparameters Tuning. *Artificial Intelligence: Theory and Applications*, Springer, 2021: 65-84.

[43] AHSAN M., GOMES R., and DENTON A. Application of a Convolutional Neural Network using transfer learning for tuberculosis detection. *Proceedings of the 2019 IEEE International Conference on Electro Information Technology* (EIT), IEEE, 2019: 427-433

[44] RUBINI C., and PAVITHRA N. Contrast enhancement of MRI images using AHE and CLAHE techniques. *International Journal of Innovative Technology and Exploring Engineering*, 2019, 9(2): 2442-2445.

[45] ALMABDY S., and ELREFAEI L. Deep convolutional neural network-based approaches for face recognition. *Applied Sciences*, 2019, 9(20): 4397.

[46] CARVALHO T., DE REZENDE E. R., ALVES M. T, *et al*., Exposing computer generated images by eye's region classification via transfer learning of VGG19 CNN. *Proceedings of the* 2017 *16th IEEE International Conference on Machine Learning and Applications* (ICMLA), IEEE, 2017: 866-870.

[47] EBERHART R., and KENNEDY J. A new optimizer using particle swarm theory. *Proceedings of the Sixth International Symposium on Micro Machine and Human Science*, IEEE, 1995: 39-43.

[48] HOUSSEIN E. H., GAD A. G., HUSSAIN K, *et al*. Major Advances in Particle Swarm Optimization: Theory, Analysis, and Application. *Swarm and Evolutionary Computation*, 2021, 63: 100868.

[49] YUSOFF M., ARIFFIN J., and MOHAMED A. DPSO based on a min-max approach and clamping strategy for the evacuation vehicle assignment problem. *Neurocomputing*, 2015, 148: 30-38.

[50] SINGH P., CHAUDHDAURY S., and PANIGRAHI B. K. Hybrid MPSO-CNN: Multi-level Particle Swarm optimized hyperparameters of Convolutional Neural Network. *Swarm and Evolutionary Computation*, 2021, 63:100863.
[51] PATHAK K. C., KUNDARAM S. S., SARVAIYA J. N, *et al*. Diagnosis and Analysis of Tuberculosis Disease Using Simple Neural Network and Deep Learning Approach for Chest X-Ray Images. In *Tracking and Preventing Diseases with Artificial Intelligence*. Springer, Cham, 2022: 77-102.
[52] ZHU Q., ZHANG P., WANG Z, *et al*. A new loss function for CNN classifier based on predefined evenly-distributed class centroids. *IEEE Access*, 2019, 8:10888-10895.
[53] PIOTROWSKI A. P., NAPIORKOWSKI J. J., and PIOTROWSKA A. E. Population size in particle swarm optimization. *Swarm and Evolutionary Computation*, 2020, 58: 100718.

参考文:

[1] NASH M.、KADAVGERE R.、ANDRADE J 等。肺结核的深度学习、计算机辅助射线照相阅读：来自印度一家三级医院的诊断准确性研究。科学报告，2020，10(1):1-10。
[2] DUONG L. T., LE N. H., TRAN T. B, et al.从胸部 X 射线图像中检测结核病：使用 视觉转换器和转移学习提高性能。具有应用程序的专家系统，2021：115519。
[3] 2019 年全球结核病报告，2021 年 1 月 22 日检索，来自 https://www.who.int/teams/global-tuberculosis-programme/tb-reports/global-report-2019。
[4] QIN Z. Z., SANDER M. S.、RAI B 等。使用人工智能读取胸片进行肺结核检测：对三个深度学习系统诊断准确性的多站点评估。科学报告，2019，9(1):1-10。
[5] DASANAYAKA C. 和 DISSANAYAKE M. B. 使用胸部 X 射线筛查肺结核的深度学习方法。生物力学和生物医学工程中的计算机方法：成像与可视化，2020:1-11。
[6] YADAV S. S. 和 JADHAV S. M. 基于深度卷积神经网络的疾病诊断医学图像分类。大数据学报, 2019, 6(1):1-18.
[7] HWANG E. J., PARK S., JIN K. N, et al.基于深度学习的胸片主要胸部疾病自动检测算法的开发和验证。美国医学会网络公开赛，2019，2(3)：e191095-e191095。
[8] KARNKAWINPONG T. 和 LIMPIYAKORN Y. 使用卷积神经网络对肺结核病变进行分类。物理学杂志：会议系列，2019，1195：012007。
[9] SENSUSIATI A. D.、PRAMULEN A. S.、RUMALA D. J 等。在印度尼西亚人的 X 射线图像中检测新冠肺炎的新方法。湖南大学自然科学学报，2021：48（6）。
[10] WANG B., SUN Y., XUE B., A 和 ZHANG M. 通过可变长度粒子群优化进化深度卷积神经网络用于图像分类。2018 年 IEEE 进化计算大会 (CEC) 的论文集 2018：1-8。
[11] SUN Y., XUE B., ZHANG M., 和 YEN G. G. 基于粒子群优化的灵活卷积自动编码器，用于图像分类。IEEE 神经网络和学习系统汇刊, 2018, 30(8): 2295-2309。
[12] ALCANTARA M. F., CAO Y., LIU B., 等。接收– 加速结核病诊断的技术进步。智能健康，2020：16。
[13] TASCI E.、ULUTURK C. 和 UGUR A. 一种基于投票的集成深度学习方法，专注于结核病检测的图像增强和预处理变化。神经计算与应用，2021：1-15。
[14] YADAV O.、PASSI K. 和 JAIN C. K. 使用深度学习对潜在结核病患者的 X 射线图像进行分类。2018 IEEE 国际生物信息学和生物医学会议 (BIBM) 论文集，2018：2368-2375。
[15] GAO X. W.、JAMES-REYNOLDS C. 和 CURRIE E. 基于增强的残差深度学习架构从计算机断层扫描肺部图像分析结核病严重程度。神经计算, 2020, 392: 233-244。
[16] YARAT S.、SENAN S. 和 ORMAN Z. 粒子群算法与其他元启发式方法的比较研究。在应用粒子群优化中，斯普林格，湛， 2021: 49-72。
[17] TIWARI H. 和 MADHUMALA R. B. 云计算中粒子群优化的回顾。用于研究和工业的智能物联网，2022：93-108。
[18] SHIRLY A. D. 、 SUDHILAYA M. 和 PRIYADHARSHINI Y 等人。使用粒子群优化技术 (粒子群算法) 提高兰兹曼直流-直流转换器的效率和功率损耗最小化。2021 年第二届新兴技术国际会议 (INCET) 论文集，IEEE，2021：1-6。
[19] 刘伟，王中，曾南，等。一种基于粒子群算法的深度学习方法，用于对急诊科患者进行分类。国际机器学习与控制论杂志，2021，12(7)：1939-1948。
[20] ESCOBAR H. 和 CUEVAS E. 使用极限学习机实现元启发式。在机器学习中的元启发式：理论与应用中，斯普林格，湛，，2021：125-147。
[21] JUNIOR F. E. F. 和 YEN G. G. 用于图像分类的深度神经网络架构的粒子群优化。群与进化计算，2019，49：62-74。
[22] 劳伦斯 T., 张 L., LIM C. P, 等。用于图像分类的自动进化卷积神经网络的粒子群优化。IEEE 访问, 2021, 9: 14369-14386。

[23] MANIKANDAN T. 和 BHARATHI N. 使用模糊自动种子聚类的肺癌检测手段形态分割和支持向量机分类器。医疗系统杂志, 2016, 40(7): 1-9

[24] KHAN A. I.、SHAH J. L. 和 BHAT M. M. 冠：一种用于从胸部 X 射线图像检测和诊断新冠肺炎的深度神经网络。生物医学中的计算机方法和程序，2020，196：105581。

[25] YU D., ZHANG K., HUANG L, 等. 胸部 X 线图像中外周插入中心导管 (PICC) 的检测：一种多任务深度学习模型。生物医学中的计算机方法和程序，2020，197：105674。

[26] SU Y.、LI D. 和 CHEN X. 基于更快的卷积神经网络框架的肺结节检测。生物医学中的计算机方法和程序，2021，200：105866。

[27] HATTIKATTI P. 使用卷积神经网络的基于纹理的间质性肺病检测。2017 年大数据、物联网和数据科学国际会议 (出价) 的论文集，IEEE，2017：18-22。

[28] ANTHIMOPOULOS M., CHRISTODOULIDIS S., EBNER L, 等。使用深度卷积神经网络对间质性肺疾病进行肺模式分类。IEEE 医学影像学报，2016，35(5)：1207-1216。

[29] LIU X.、LEI H. 和 HAN S. 使用卷积神经网络从计算机断层扫描中检测结核病。计算机断层扫描的进展, 2019, 08(04): 47–56。

[30] HOODA R.、SOFAT S.、KAUR S 等。深度学习：一种使用胸片检测结核病的潜在方法。 2017 年 IEEE 信号和图像处理应用国际会议 (ICSIPA) 的论文集， IEEE，2017：497-502。

[31] RAJARAMAN S., CANDEMIR S., XUE Z, 等。用于改进胸片中结核病检测的模型的新型堆叠概括。2018 年第 40 届 IEEE 医学与生物学工程学会 (欧洲商业银行) 国际会议论文集，IEEE，2018：718-721。

[32] ABIDEEN Z. U.、GHAFOOR M.、MUNIR K 等。不确定性有助于使用贝叶斯卷积神经网络进行稳健的结核病识别。IEEE 访问，2020 年，第 8 期：22812-22825。

[33] CAO Y., LIU C., LIU B, 等。在资源匮乏和边缘化社区中使用深度学习和移动医疗技术改进结核病诊断。2016 IEEE 首届互联健康国际会议论文集：应用、系统和工程技术（追赶），IEEE，2016：274-281。

[34] SHIN H. C., ROTH H. R., GAO M, 等。用于计算机辅助检测的深度卷积神经网络：美国有线电视新闻网架构、数据集特征和迁移学习。IEEE 医学影像学报，2016，35(5)：1285-1298。

[35] TAJBAKHSH N.、SHIN J. Y.、GURUDU S. R. 等。用于医学图像分析的卷积神经网络：全面训练还是微调？IEEE 医学影像学报，2016，5(5)：1299-1312。

[36] LIU C., CAO Y., ALCANTARA M, 等。德克萨斯-美国有线电视新闻网：使用卷积神经网络检测胸部 X 射线图像中的结核病。国际图像处理会议论文集，国际知识产权中心，2018：314-318。

[37] KERMANY D. S., GOLDBAUM M., CAI W., 等。通过基于图像的深度学习资源识别医学诊断和可治疗疾病通过基于图像的深度学习识别医学诊断和可治疗疾病。细胞, 2018, 172(5): 1122-1131。

[38] RAHMAN T.、KHANDAKAR A.、KADIR M. A. 等。使用深度学习、分割和可视化的胸部 X 射线进行可靠的结核病检测。 IEEE 访问, 2020, 8: 191586-191601。

[39] DIAS JÚNIOR D. A.、DA CRUZ L. B.、BANDEIRA DINIZ J. O 等。使用深度特征和粒子群算法优化的 XGBoost 基于胸部 X 射线图像对新冠肺炎患者进行分类的自动方法。具有应用程序的专家系统，2021：183。

[40] 加斯帕 A.、奥利瓦 D.、库瓦斯 E. 等。使用元启发式算法的卷积神经网络中的超参数优化。在机器学习中的元启发式：理论和应用。斯普林格，查姆。 2021：37-59。

[41] FOYSAL M. F. A.、SULTANA N.、RIMI T. A. 和 RIFAT M. H. 使用粒子群优化的卷积神经网络超参数优化。在数据挖掘和信息安全的新兴技术中，斯普林格，新加坡，2021：363-373。

[42] TUBA E.、BAČANIN N.、STRUMBERGER I. 和 TUBA M. 卷积神经网络超参数调整。人工智能：理论与应用，斯普林格，2021：65-84。

[43] AHSAN M.、GOMES R. 和 DENTON A. 使用迁移学习进行结核病检测的卷积神经网络的应用。2019 IEEE 国际电子信息技术会议 (EIT) 论文集，IEEE，2019：427-433

[44] RUBINI C. 和 PAVITHRA N. 使用 AHE 和克拉赫技术增强核磁共振图像的对比度。国际创新技术与探索工程杂志, 2019, 9(2): 2442-2445.

[45] ALMABDY S. 和 ELREFAEI L. 基于深度卷积神经网络的人脸识别方法。应用科学, 2019, 9(20): 4397。

[46] CARVALHO T., DE REZENDE E. R., ALVES M. T, 等。通过 VGG19 美国有线电视新闻网的迁移学习，通过眼睛

区域分类暴露计算机生成的图像。 2017 年第 16 届 IEEE 机器学习与应用国际会议 (ICMLA) 的论文集，IEEE，2017：866-870。

[47] EBERHART R. 和 KENNEDY J. 使用粒子群理论的新优化器。第六届微型机械与人类科学国际研讨会论文集，IEEE，1995：39-43。

[48] HOUSSEIN E. H.、GAD A. G.、HUSSAIN K 等。粒子群优化的主要进展：理论、分析和应用。群与进化计算，2021，63：100868。

[49] YUSOFF M.、ARIFFIN J. 和 MOHAMED A. DPSO 基于最小-最大方法和疏散车辆分配问题的钳位策略。神经计算，2015，148：30-38。

[50] SINGH P.、CHAUDHDAURY S. 和 PANIGRAHI B. K. 混合 MPSO-美国有线电视新闻网：卷积神经网络的多级粒子群优化超参数。群与进化计算，2021，63：100863。

[51] PATHAK K. C.、KUNDARAM S. S.、SARVAIYA J. N 等。使用简单神经网络和深度学习方法对胸部 X 射线图像进行结核病诊断和分析。在使用人工智能跟踪和预防疾病方面。斯普林格，湛，2022：77-102。

[52] 朱强，张平，王 Z，等。基于预定义均匀分布的类质心的美国有线电视新闻网分类器的新损失函数。IEEE 访问，2019，8:10888-10895。

[53] PIOTROWSKI A. P.、NAPIORKOWSKI J. J. 和 PIOTROWSKA A. E. 粒子群优化中的种群大小。群与进化计算，2020，58：100718。